나노임프린트리소그래피의 엠보싱 과정에서의 흐름거동

정준호, 최윤석*, 신영재, 이재종, 박경택, 이상록, 이응숙
한국기계연구원, 지능형정밀기계연구부
경원테크*

Flow behavior at the embossing stage of nanoimprint lithography

Jun-Ho Jeong, Youn-Suk Choi*, Young-Jae Shin, Jae-Jong Lee, Kyoung-Taik Park, Eung-Sug Lee, and Sang-Rok Lee
Korea Institute of Machinery and Materials, Department of Intelligent Precision Machine
KyungWon Tech Corporation*

Introduction

The nanoimprint lithography (NIL)[1] process consists of two stages: the embossing stage and the anisotropic etching stage. In the embossing stage, a stamp with nano/micro scale structures is pressed into a thin polymer layer on a substrate, and then is separated from the layer. To minimize air entrapment, the embossing process should be done in a vacuum. During the anisotropic etching stage, the residual polymer is removed completely in the compressed area.

In this study, through numerical experimentation, we present the effects of capillary force and width of stamp groove on flow behavior at the embossing stage. We also compare our numerical results with previous experimental results and discuss physical phenomena at the embossing stage. A commercial computational fluid dynamics (CFD) code based on the finite volume method (FVM), CFD-ACE, is used for simulating filling behavior. In the code, an unsteady incompressible flow with free surfaces is solved on the Eulerian grid by using the full Navier-Stokes momentum equation and the volume of fluid (VOF) method. In order to consider surface tension effects, the high-order nonlinear boundary conditions on a fluid surface are also imposed on free surfaces.

Computational methods

Chan and Horn[2] proposed that the Reynolds description of the drainage process for organic liquids appears to be very accurate down to film thickness of about 50nm. They also showed that the continuum hypothesis breaks down, as the film thickness is less than about ten molecules thick. The dimensions of a polymer molecule-chain are usually characterized by the radius of gyration, R_g, defined as the square root of the average squared distance of all the repeating units of the chain from the center of the mass of the chain. Jackson et al.[3] presented the relation between R_g and molecular weight of the polymethylmethacrylate (PMMA) in tetrahydrofuran (THF) at room temperature as follows:

$$R_g = 0.012M^{0.583} \tag{1}$$

where M is the molecular weight. From the above relation, we obtain the value R_g=8.34nm for the PMMA with M =75,000g/mol as used in Heydermann et al.'s experiment[4]. Based on Chan and Horn's results and the value of the R_g computed, we assume that a PMMA of M =75,000g/mol satisfies the continuum hypothesis as $L \geq 100nm$. This study is focused on understanding physical phenomena in embossing nano/micro scale structures with 100nm minimum feature size through numerical simulation under the continuum hypothesis. In this study, a computational method based on the semi-implicit pressure-linked equation algorithm (SIMPLE)[5] is employed for solving the continuity and Navier-Stokes momentum equations:

Numerical results

In this numerical experiment, we used the PMMA as a resist material in order to compare our results with Heydermann et al.'s experimental results. To simplify our numerical studies we assumed that the embossing stage is isothermal and a stamp moves down with a constant velocity. The density used is 1.17×10^3kg/m^3[6], viscosity is 3.00×10^3 Pa s[4], surface tension is 29.7 mN/m[7], and wetting angle is 25°. The geometry of the computational domain including the stamp and boundary conditions are shown in Figure 1. Assuming that the polymer melt is incompressible and $S >> h_f$ and h_o, the embossing speeds V_e are computed from the equation [4]

$$V_e = (h_o - h_f)/t_f = 2ph_f^2 h_o^2 / \left(\mu S^2 (h_o + h_f)\right) \qquad (2)$$

where h_0 is the initial height of the polymer film, h_f is the final height of the polymer film which is given by $h_f = h_o - WD/(S+W)$, μ is the viscosity, W is the width of stamp groove, D is the depth of stamp groove, S is the width of stamp, and p is the embossing pressure. For all case studies, the embossing speeds computed from Eq. (2) are given in Table 1. Because the embossing process is done in a vacuum, the effect of air pressure can be neglected. In order to make the air flow out, we created an artificial outlet with the width $D_0 \approx D/50$ at the middle of the top of the cavity.

In Figure 2, we compare our numerical results with Heydermann et al.'s experimental results for the PMMA with M =75,000g/mol. Figure 2(a) shows numerical results for S =60μm and W =20μm that correspond to the atomic force microscope (AFM) height profiles[4], respectively. It is shown that the predicted free surface shapes are in excellent agreement with the experimental results. The characteristic length L for this case has a range from 156.25nm to 200nm because h_0 is equal to 200nm and the maximum pressing distance of the stamp is 43.75nm. It is shown from the result that the simulation of the embossing stage under the continuum hypothesis is reasonable at the 100nm length scale.

Figure 3 shows the obvious effect of the capillary force on filling behavior. The PMMA melt is completely filled at the corner of the cavity in Figure 3(a), but it is not filled at the corner in Figure 3(b). The interface between region B and air is almost vertical in Figure 3(a), while the interface is inclined at about 30° to the vertical in Figure 3(b). We can also see the concave region only in Figure 3(a). Figure 3(c) shows that the concave region is formed by the capillary force. For the simulation with no embossing speed, the interface does not move from 1.40sec and keeps its position because there is no inflow from outside.

In order to understand three-dimensional (3D) flow behavior at the embossing stage, a 3D simulation for S =30μm and W =10μm was carried out. The simulation results are compared with the 3D AFM images[4] for S =60μm and W =20μm in Figure 4. The predicted free surface shapes are in good agreement with the experimental results, even though the domain size of the simulation is different from that of the experiment.

To investigate the effect of width of stamp groove on flow behavior, we also simulated cases of W =1μm and W =100nm. In both cases, the S is given as 30μm as with the case of the W =10μm. It is shown that the free surface shape is dramatically changed according to the groove width in Figures 3, 5, and 6. Figure 5(a) shows that the free surface shape for the case of W =1μm maintains a single curved shape and has no local concave region. This result occurs because the W used is too small to make a double-well shape through surface tension alone as shown in Figure 5(c) and the distance between the two peaks of two-humped shape created only by viscous flow is too short as shown in Figure 5(b). In the case of W =100nm, the free surface has a totally convex interface as shown in Figure 6. The reason for this result is that the W used is too small to make a two-humped shape by viscous flow

as shown in Figure 6(b) and the viscous flow is much faster than the capillary flow due to the high embossing speed and small groove width to be used for the simulation.

Conclusions

In order to understand physical phenomena in embossing nano/micro-scale structures with 100nm minimum feature size, a numerical experiment using a commercial CFD code, CFD-ACE, has been carried out. Through the comparison between our numerical result and Heydermann et al.'s experimental result, it has been shown that the numerical simulation of the embossing stage under the continuum hypothesis is reasonable at a 100nm length scale. Through several numerical case studies, we have also presented that the flow behavior in the embossing stage is dominantly affected by the capillary force and width of stamp groove.

References

1. S.Y. Chou, P.R. Krauss, W.Zhang, L. Guo, L. Zhuang, *J. Vac. Sci. Technol. B* **15** 2897 (1997).
2. D. Y. C. Chan and R. G. Horn, *J. Chem. Phys.*,**83** 5311 (1985).
3. C. Jackson, Y.J.Chen, and J.W. Mays, *J. Appl. Polym Sci.* **61** 865 (1996).
4. L.J. Heydermann, H. Schift, C. David, J. Gobrecht, and T. Schweizer *Microelectronic Engineering*, **54** 229 (2000).
5. S. Parakar, "Numerical heat transfer and fluid flow", Heisphere Publishing Corp., New York: McGraw Hill, 1980.
6. Z. Tadmor and C. Gogos, "Principles of polymer processing", Wiley New York, 1970.
7. E. Schaffer, "Instability in thin polymer films: structure formation and pattern transfer", Ph.D. thesis, University of Groningen, 2001.

Dimension	S(μm)	W(μm)	p (Pa)	D (nm)	h_0 (nm)	h_f (nm)	V_e (nm/sec)
2D	60	20	3.6×10^6	175	200	156.25	1.83
2D	30	10	3.6×10^6	175	200	156.25	7.31
2D	30	1	3.6×10^6	175	200	194.35	10.2
2D	30	0.1	3.6×10^6	175	200	199.42	10.6
3D	30	10	6.7×10^5	175	200	189.06	1.83

Table 1 Simulation conditions for all cases

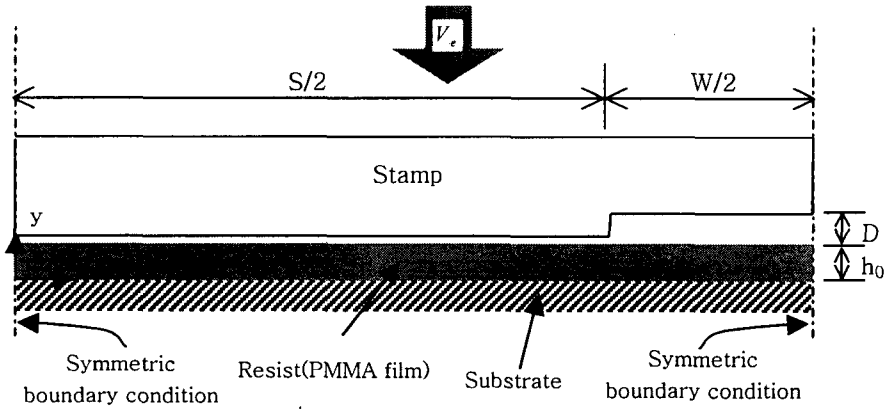

Figure 1 The geometry of computation domain and boundary conditions

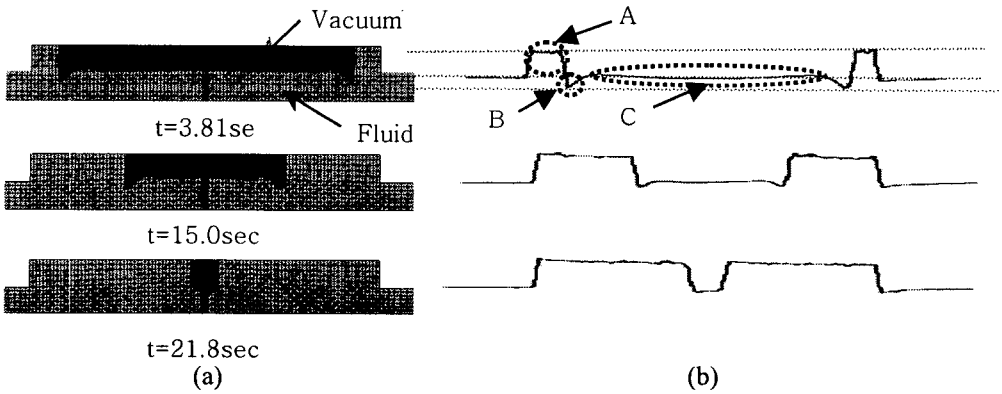

Figure 2 Comparison of 2D simulation results(a) and AFM height profiles(b)[4]

(a) for σ=29.7mN/m and V_e=7.31nm/s at t=2.41sec

(b) for σ=0 and V_e=7.31nm/s at t=2.46sec

c) for σ=29.7mN/m and V_e=0 at t=2.44sec

Figure 3 Predicted free surface shapes for W=10μm

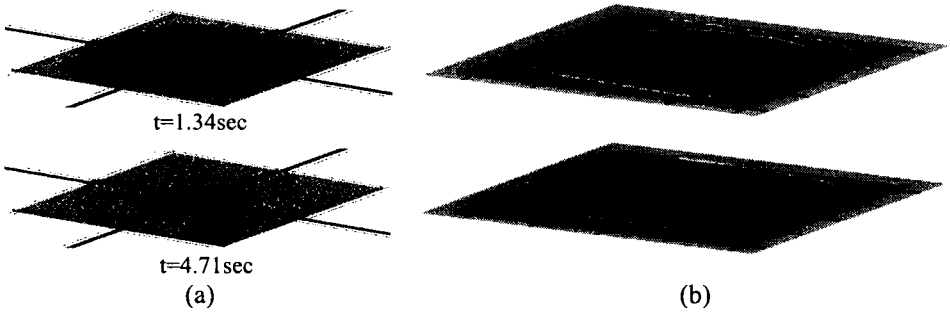

Figure 4 Comparison of 3D simulation results(a) and 3D AFM height profiles(b)[4]

(a) for σ=29.7mN/m and V_e=10.2nm/s at t=0.220sec

(b) for σ=0 and V_e=10.2nm/s at t=0.236sec

(c) for σ=29.7mN/m and V_e=0 at t=0.276sec

Figure 5 Predicted free surface shapes for W=1μm

(a) for σ=29.7mN/m and V_e=10.6nm/s at t=0.0275sec

(b) for σ=0 and V_e=10.6nm/s at t=0.0259sec

c) for σ=29.7mN/m and V_e=0 at t=0.0288sec

Figure 6 Predicted free surface shapes for W=100nm